Partial Activation of the Insulin Receptor Kinase Domain by Juxtamembrane Autophosphorylation†

Aaron Darius Cann, Steven M. Bishop, Ararat J. Ablooglu, and Ronald A. Kohanski*

Department of Biochemistry, Box 1020, The Mount Sinai School of Medicine, 1 Gustave L. Levy Place, New York, New York 10029

Received April 21, 1998; Revised Manuscript Received June 16, 1998

ABSTRACT: Increased enzymatic activity of receptor tyrosine kinases occurs after trans-phosphorylation of one or two tyrosines in the activation loop, located near the catalytic cleft. Partial activation of the insulin receptor's kinase domain was observed at dilute concentrations of kinase, suggesting that cis-autophosphorylation was occurring. Autophosphorylation during partial activation mapped to the juxtamembrane (JM) tyrosines and not to activation loop tyrosines. Furthermore, a double JM Tyr-to-Phe mutant kinase (JMY2F) did not undergo partial activation but catalyzed substrate phosphorylation at a very low rate. Steady-state kinetics of peptide phosphorylation were determined with and without JM autophosphorylation. The JMY2F mutant was used to prevent concurrent cis-autophosphorylation and therefore to approximate the basal state apoenzyme in the kinetic analysis. Partial activation was dominated by a decreased Michaelis constant for peptide substrate, from $K_{M,PEP} \geq 2.5$ mM in the basal state to 0.2 mM in the partially activated state; the $K_{M,ATP}$ remained virtually unchanged at ∼1 mM, and k_{cat} increased from 180 to 600 min^{-1}. The high $K_{M,PEP}$ suggests weak binding of peptide substrates to the apoenzyme. This was confirmed by $K_i > 1$ mM for peptide substrates used as inhibitors of JM autophosphorylation. The absence of comparably large changes in k_{cat} and $K_{M,ATP}$ suggests that the JM region is primarily a strong barrier to the peptide entry step of trans-phosphorylation reactions. The JM region therefore functions as an intrasteric inhibitor in the basal state of the insulin receptor's kinase domain.

Protein kinases are members of a highly conserved family of enzymes. They have characteristic basal and activated states defined by low and high catalytic efficiencies, respectively. The ability to switch between these states in response to diverse signals provides a fundamental mechanism for regulation of metabolic and signaling pathways. In this context, protein kinases have evolved as individual proteins, as subunits of ensembles, and as domains of larger macromolecules. Every protein kinase has a catalytic "core" of ∼300 amino acids recognizable by the extraordinary sequence conservation across both serine/threonine and tyrosine kinase subfamilies (*1*). The bilobal architecture of this core and the active site, situated in the cleft between the N-terminal[1] small lobe and the C-terminal large lobe, are also conserved, as demonstrated by the crystal structures published to date. A segment of 6−20 amino acids from the large lobe of the conserved core forms an "activation loop" or "T-loop" that is structurally and functionally associated with the active site cleft. Although present in the majority of protein kinases, these activation loops show little sequence similarity between kinase families and are often not well conserved even within one kinase family. Activation loops frequently include a phosphorylated residue that can be an important determinant in basal and activated states of the kinase (cf. Owens (*2*) for summary). Because the core includes all the functional groups required for phosphoryl transfer, conformational changes and reversible chemical modifications within the conserved core and the variable activation loop should be responsible for determining the level of catalytic efficiency. However, as illustrated by the following examples, domains outside the core impact kinase conformation, susceptibility to regulatory modification, and catalytic efficiency.

Src family kinases are single polypeptide chains divided into discrete domains. The amino-terminal myristoylation sequence is followed by an SH3 domain, an SH2 domain, the conserved core, and a C-terminal tail including an important tyrosine phosphorylation site. The activation loop contains a tyrosine phosphorylation site that also affects kinase activity. Within a single c-Src kinase molecule, interaction of the C-terminal phosphotyrosine with the N-terminal SH2 domain maintains the cellular Src kinases in their basal states (*3*). The molecular basis for this cis-inhibition arises either from restrictions on the core's mobility

† Supported by Grant DK50074 from the National Institutes of Health.

* To whom correspondence should be addressed. Phone: (212)-241−6897. Fax: (212)-996-7214. E-mail: r_kohanski@smtplink.mssm.edu.

[1] Abbreviations: Ac, acetate; AL, activation loop; CamK, Ca^{2+}/calmodulin-dependent protein kinase; C subunit, catalytic subunit of the cyclic-AMP dependent protein kinase; C-terminal, carboxy-terminal; DTT, dithiothreitol; EDTA, ethylenediaminetetraacetic acid; IR, insulin receptor; IRS-1, insulin receptor substrate-1; JM, juxtamembrane; JMY2F, double $Tyr^{965,972}$-to-Phe mutant of the KD; KD, kinase domain of the human insulin receptor; N-terminal, amino-terminal; PAGE, polyacrylamide gel electrophoresis; PKA, cyclic-AMP-dependent protein kinase; PTB, protein tyrosine binding domain; PTyr, phosphotyrosine; R subunit, regulatory subunit of the cyclic-AMP-dependent protein kinase; RTK, receptor tyrosine kinase; SDS, sodium dodecyl sulfate; SH2 (3), Src homology domain-2 (−3); Tris, tris(hydroxymethyl)aminomethane.

S0006-2960(98)00912-X CCC: $15.00
Published on Web 07/25/1998

and the dislocation of catalytically essential residues because the SH3 domain impinges on the small lobe of the core (*4*), or from simple steric occlusion of the SH2 or SH3 domains required for efficient substrate protein recruitment (*5*). Partial activation requires displacement of the endogenous PTyr-containing C-terminal sequence with an alternative ligand (*6*) or by dephosphorylation (*7*). Maximal activation requires phosphorylation of a regulatory tyrosine in the activation loop which seems to relieve a second layer of intrasteric inhibition at the catalytic cleft, and may also promote alignment of specific residues involved in phosphoryl transfer. Therefore the basal state of Src family kinases is maintained by amino- and carboxy-terminal domains, and modifications within the activation loop are required for maximal activation.

There are multiple motifs for maintaining the basal state of Ca^{2+}/calmodulin-dependent protein kinases (CaMKs). The basal state of CaMK I arises from a combination of "noncompetitive" inhibition against ATP binding and "competitive" inhibition against peptide binding, both from interactions between the carboxy terminus and the catalytic core (*8*). Truncations of the carboxy terminus by limited proteolysis (*9*, *10*) or by mutagenesis (*11*−*14*) have elucidated most of the important regions required for cis inhibition and Ca^{2+}/CaM binding. This binding can be inhibited or enhanced by phosphorylations near the Ca^{2+}/CaM binding region, either blocking activation or prolonging activation after Ca^{2+}/CaM release in CaMK II, depending on the specific threonine phosphorylated (*15*). In addition, an AMP-dependent or other Ca^{2+}/CaM-dependent protein kinase can phosphorylate a threonine in the activation loops of CaMK I or IV and subsequently augment the activation resulting from Ca^{2+}/CaM binding (*16*−*18*). In both the Src and CaMK families reversible, ligand-regulated, and phosphorylation-dependent partial activation has been demonstrated. Equally significant is the role of amino- and carboxy-terminal regions in altering the susceptibility of activation loop Thr or Tyr residues toward phosphorylation as a molecular mechanism for maximizing catalytic efficiency.

The cyclic-AMP-dependent protein kinase (PKA) is inhibited by interactions between the regulatory and catalytic subunits (R and C subunits, respectively) which form the basal state holoenzyme (*19*) and between the C subunit and PKI, the heat-stable inhibitor (*20*). Binding of the R subunit and PKI is dependent on their substrate-like consensus sequences (*21*−*23*), but the R subunits' binding is also dependent on phosphothreonine-197 (*24*) whereas PKI binding is dependent more on other features (*25*). This phosphothreonine, in the activation loop, appears to be constitutively phosphorylated and thus does not undergo rounds of phosphorylation and dephosphorylation as regulatory events (*26*). However, PThr-197 is critical for efficient function of the C subunit in the activated state that results from dissociation of the R subunit, and therefore serves important roles in maintaining both the basal and activated states (*24*, *26*). In addition, the amino-terminal 40 residues of mammalian PKA interact with the catalytic core (*27*). Selective mutagenesis demonstrated only a minor role for determining catalytic efficiency in the activated free C subunit. However there were significant changes in the interaction between the C subunit and class I, not class II, R subunits (*28*). Therefore, the amino-terminal region adds another layer of regulation to the basal state of PKA. Furthermore, residues in the C-terminal core-flanking region of PKA can significantly alter catalytic efficiency (*29*).

As these three examples demonstrate, activation of soluble protein kinases requires direct physical interactions between the catalytic core and regulatory domains, subunits, or proteins. Receptor tyrosine kinases (RTKs) present an additional challenge because the principle regulatory domain, the ligand binding domain or subunit, is separated from the cytoplasmic kinase domain by the plasma membrane. The generalized molecular solution to this problem is regulation through ligand-induced aggregation of at least two transmembrane components which results in contacts on the intracellular side of the membrane. The special solution employed by monomeric RTKs—with a single ectodomain for ligand binding and a single endodomain with low basal enzymatic activity—is ligand-induced dimerization leading to direct contact between kinase domains. The resulting trans-autophosphorylation either elevates kinase activity, creates new sites for interaction with other signaling molecules, or both. In this regulatory scheme the basal state apoprotein is easily maintained because the effective concentrations of intracellular kinase domains are too low for frequent and/or efficient trans-phosphorylation to be significant, that is, sufficient to overcome reversal by phosphatases.

The unique challenge of maintaining a basal state for the insulin receptor is imposed by its native structure, an $\alpha_2\beta_2$ heterotetramer. This "pre-dimerized" state leads to the constitutive proximity of the receptor's two intracellular kinase domains, even in the absence of insulin. It may be assumed that insulin-induced conformational changes lead to trans-autophosphorylation of the kinase domains, and there is evidence for insulin-induced changes in the β-subunit following insulin binding to the α-subunit in the native receptor (*30*−*33*). In mechanistic terms, this assumption means either the kinase domains are too far apart in the unliganded insulin receptor to interact, or there is another layer of cis-inhibition that restricts the trans-reaction. Under either possibility, there must be an intracellular subdomain of the β-subunit that first reacts to the binding of insulin, before the first autophosphorylation occurs, and is therefore instrumental in orchestrating the transition from a basal to an activated kinase. We have recently established that juxtamembrane tyrosines of the insulin receptor react by a cis-mechanism and the reaction takes place in the absence of autophosphorylation in the core or carboxy-terminal regions (*34*). In this study we present the first evidence supporting intrasteric inhibition by the juxtamembrane region of the unphosphorylated insulin receptor's kinase domain. Together with evidence indicating the early reaction of juxtamembrane tyrosines in response to insulin (*35*, *36*), this suggests a novel regulatory role for the juxtamembrane region in the basal state of the insulin receptor. Thus, the IR may incorporate regulatory motifs described previously for soluble protein kinases and utilize regions outside of the catalytic core to control activation of its kinase domain.

EXPERIMENTAL PROCEDURES

Materials. ATP (disodium salt from Equine muscle), insulin-free radioimmunoassay-grade Fraction V bovine serum albumin (BSA), and grade V protamine chloride from salmon were from Sigma; electrophoresis, thin-layer chro-

matography, and HPLC reagents were from Fisher; insect cell culture reagents were from Gibco/BRL; X-ray film and cellulose thin-layer plates (Eastman 13255) were from Kodak; [^{32}P]orthophosphate was from ICN; and [γ-^{32}P]ATP was synthesized by the method of Walseth and Johnson (*37*) and purified (*38*). Peptides were synthesized using Fmoc chemistry, HPLC-purified, and confirmed by amino acid analysis and automated Edman degradation by Dr. Imre Wolf of Mount Sinai's Protein Chemistry Core.

Recombinant Cytoplasmic Kinase Domain Cloning, Expression, and Purification. Baculovirus encoding amino acid residues 953−1355 of the wild-type KD was a generous gift of the late Dr. Ora Rosen (*39*); the numbering is from Ebina et al. (*40*). The Tyr^{965,972}Phe double mutant, JMY2F, was subcloned as described previously (*34*) using the 3′ end of the human insulin cDNA isolated from the vector pTZ19U-IR, kindly provided by Dr. J. Whittaker (*41*). The recombinant virus was generated using the BaculoGold system from Pharmingen. Wild-type and mutant KD were expressed in Hi5 cells infected at an MOI of 3−5 for 46−48 h. Purification was done by a modification of Villalba et al. (*39*) as described earlier (*34*) with the addition of strong anion-exchange chromatography as a final step. We used a DEAE-8HR (Waters), a Superdex 75 (16/60 or 26/60; Pharmacia), and a 1 mL MonoQ (Pharmacia) or 2 mL Q-column (Waters) in that order. Ion-exchange columns were developed with linear gradients in NaCl. The buffer was 50 mM Tris HCl, pH 7.4 (adjusted at room temperature but used at 4 °C). KD was detected by Western blot with rabbit polyclonal anti-KD antibodies (prepared in collaboration with Dr. Lu-Hai Wang). Purity was confirmed to be at least 98% with ≥10 μg of KD/lane by SDS−PAGE, nondenaturing PAGE, and silver staining using the method of Ansörge (*42*). Purified proteins were quantified spectrophotometrically at 280 nm (for wild-type KD, $\epsilon = 40\,200$ M^{-1} cm^{-1} and for JMY2F, $\epsilon = 37\,800$ M^{-1} cm^{-1}). The purified proteins were stored at −20 °C in 30% glycerol (v/v).

Kinase Domain Autophosphorylation. To assess inhibition of autophosphorylation by peptide substrates, one minute reactions were done at 0.1 μM KD, 10 μM [γ-^{32}P]ATP, 5 mM $MnAc_2$, 50 mM TrisAc, pH 7. Reactions were quenched by the addition of one-half volume of 3×-concentrated SDS−PAGE sample buffer and the products resolved by SDS−PAGE on 12.5% acrylamide gels by the method of Laemmli (*43*). The ^{32}P-labeled KD was located by autoradiography and the excised KD was quantified by Cerenkov counting. All reactions were done in duplicate. Peptides were present at 0.1 or 1.0 mM, or without peptide as the control reaction condition.

Steady-State Kinetics of Peptide Phosphorylation. The peptide IRS939 (see below) was used for steady-state kinetics. Phosphorylation was analyzed by the HPLC-based assay (*44*) except that in the present study quantification of apo- and phosphopeptides was done by peak area integration. All reagents were titrated to pH 7.0 ± 0.2, and reactions were performed at room temperature in 20 or 50 mM $MgAc_2$, 50 mM TrisAc, pH 7.0 with 0.05 mg of BSA/mL as carrier. The JMY2F mutant was used for the basal state apoenzyme. Peptide phosphorylation was done at a final concentration of 0.1 μM KD. The reaction times were varied between 5 and 30 min, depending on the peptide and ATP concentrations. These covered the ranges 0.2−3.0 mM IRS939 and 0.2−5 mM ATP. Three time points were taken for each pair of peptide and ATP concentrations, in duplicate, and the rate was determined as the slope of micromolar phosphopeptide formed versus time. JM-autophosphorylated wild-type KD was generated by a 30 min reaction with 0.2 μM KD, 0.2 mM ATP, 20 mM $MgAc_2$. Aliquots were diluted 10-fold into peptide phosphorylation reaction mixtures to give 20 nM JM-phosphorylated KD; the ATP concentration was adjusted to include the dilution from the pre-autophosphorylation reaction. Peptide concentrations were over the range 0.02−1.0 mM IRS939, and ATP was varied between 0.2 and 4 mM. The reaction times varied between 2 and 24 min. Rates were calculated as described above. Steady-state kinetic parameters were extracted from Lineweaver−Burk and from Eadie−Scatchard plots; the agreement between these graphical methods was within 20%. The V_{max} and K_M values were determined from secondary plots of the appropriate intercepts and slopes.

Non-Denaturing Polyacrylamide Gel Electrophoresis. To monitor relative phosphorylation by increased electrophoretic mobility, we used nondenaturing PAGE under the following conditions: Kinase domain autophosphorylation was done using 0.1% hydrogenated Triton X-100 (CalBiochem) instead of carrier BSA because the electrophoretic mobility of BSA coincided with near-maximally autophosphorylated KD (not shown). The reactions at 20 mM $MgAc_2$ were quenched by adding 1.2 volumes of 75 mM Tris HCl, 40 mM EDTA, 20 mM DTT, 20% glycerol (v/v), and 0.01% bromphenol blue, pH 6.65 (titrated before adding the dye). Samples were cooled immediately on ice. Slab gels of 0.75 mm thickness were cast and run using a Hoeffer (Pharmacia) SE 600 system, and the depth of the wells was 10 mm instead of 30 mm; deeper wells produce more of a "dumbbell" appearance in the stained protein bands. The acrylamide concentration was 8.5% T (3% C), and the gel composition was the same as a standard Laemmli gel (*43*) but without the SDS, and the final Tris HCl concentration was 0.25 M instead of 0.375 M. The stacking gel was 5% T (3% C), and the Tris HCl concentration was a standard 0.125 M. The gel was used the same day it was cast, and was precooled to 5 °C; temperature was maintained using a Brinkman recirculating water bath. After loading the samples, the gel was run at 200v for 4 h. The protein bands were visualized by silver staining using the method of Ansörge (*42*).

Other Methods. Phosphopeptide mapping was done by the method of Boyle et al. (*45*) with modifications, as described previously (*34*). Autoradiograms were scanned on an Arcus II scanner (Agfa) and the figures prepared using Adobe Photoshop. Computer-generated curves presented in the figures were made and plotted using Microsoft Excel.

Synthetic Peptides. The names and amino acid sequences of synthetic peptides (free acid at the carboxy termini) derived from the sequences of IRS-1 or SHC and used in this study are the following: IRS939, REETGSEEYMNMDLG; Firs939, REETGSEEFMNMDLG; IRS1172, GLEKSLNYIDLDL; SHC317, RELFDDPSYVNVQNLD.

RESULTS

Weak Inhibition of Cis-Autophosphorylation by Peptide Substrates. The insulin receptor's kinase domain is activated

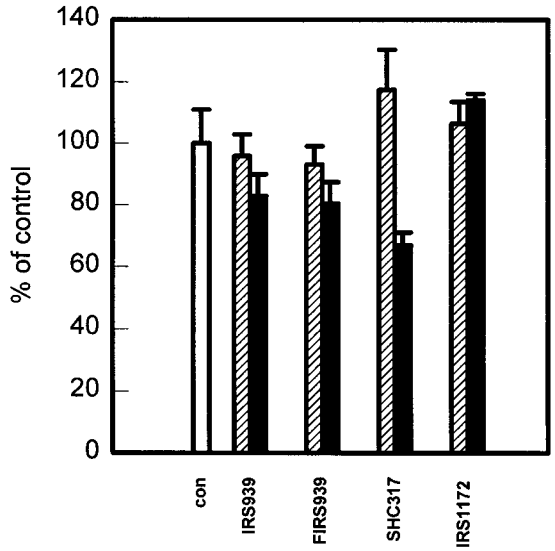

FIGURE 1: Inhibition of insulin receptor kinase domain by peptide substrates and substrate analogues. Autophosphorylation of 100 nM wild-type KD was done for 1 min at 10 μM [γ-^{32}P]ATP (20 000 cpm/pmol), 5 mM $MnAc_2$, pH 7.0 in the absence (control) or presence of 0.1 or 1.0 mM peptide substrate or substrate analogue (hatched and solid bars, respectively). The autophosphorylated KD was resolved by SDS−PAGE and the phosphorylation determined by Cerenkov counting, as described in the text. Net ^{32}P−KD for the control was 3650 ± 410 cpm, and the results are reported as percent of control. Amino acid sequences of these peptides are given at the end of the Experimental Procedures.

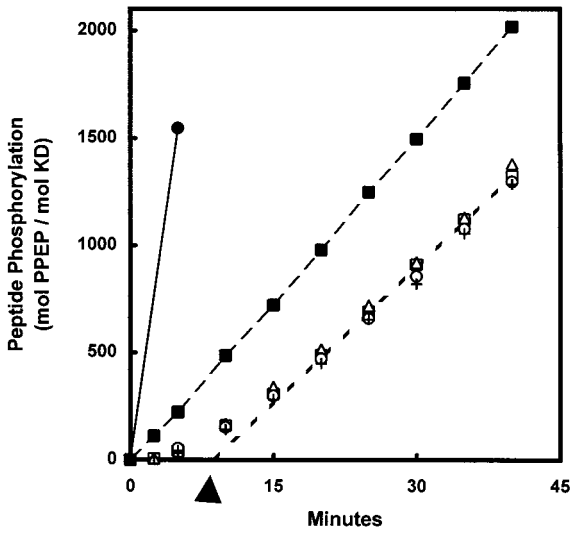

FIGURE 2: Progressive kinase activation under cis-autophosphorylation reaction conditions. Peptide phosphorylation of IRS939 by wild-type KD was measured over a 40 min time course, after or without preincubation of the KD with selected components of the final reaction. The final reaction conditions were 5 nM wild-type KD, 50 mM $MgAc_2$, 0.5 mM ATP, 50μM IRS939, in buffer (50 mM TrisAc, pH 7.0, with 0.1 mg of BSA/mL). Preincubation of 500 nM KD for 25 min was done under the following conditions: control, no additions (□); 50 μM IRS939 (△); 0.5 mM $MgAc_2$ (○); 2 mM AMP−PNP plus 50 mM $MgAc_2$ (+); 0.5 mM ATP plus 50 mM $MgAc_2$ (■); 0.5 mM ATP, 50 mM $MgAc_2$ plus protamine at 0.05 μg/mL (●). The induction time was determined by linear extrapolation from the apparent steady state to 0 product formed (arrowhead). Further details are given in the text.

by autophosphorylation. Because autophosphorylation is concurrent with peptide substrate phosphorylation, characterization of substrate phosphorylation by the apoenzyme has been problematic. Earlier attempts to assess substrate phosphorylation by the apoenzyme relied on saturating substrate concentrations to serve as competitive inhibitors of autophosphorylation, with the intention of preserving the basal state. Proteins and Glu-Tyr copolymers were used in that earlier work, and in some cases there was "residual" autophosphorylation, even at the highest substrate concentrations. On the basis of the use of small peptide substrates with low K_M values as reported by Shoelson et al. (*46*), we screened several synthetic peptide substrates for one that would be a strong inhibitor of the "residual" autophosphorylation. These peptides were derived from likely phosphorylation sites in IRS-1 (*46*) and also in SHC (*47*). In addition, we presumed that residual autophosphorylation observed in the above studies should map to the JM region of the kinase because low ATP concentrations had been employed, and low ATP concentrations favor the cis-reaction of JM tyrosines (*36*, *48*). Therefore we tested peptide substrates and one Phe-for-Tyr analogue as inhibitors of cis-autophosphorylation in the recombinant cytoplasmic kinase domain of the insulin receptor. As shown in Figure 1, we found only very weak inhibition even at millimolar concentrations of peptide. This was surprising in light of the $K_M \approx 24$ μM reported for a similar peptide (*46*). We would not have expected weak inhibition of JM autophosphorylation unless JM tyrosine(s) was (were) bound more strongly in the active site than these "good" substrates, whether or not another competitor for the active site is available. Following this logic in reverse, the JM region should have an inhibitory effect on peptide substrate phosphorylation and consequently JM autophosphorylation might activate the kinase.

Partial Kinase Activation during Cis-Autophosphorylation. Peptide substrate phosphorylation was analyzed under cis-autophosphorylation reaction conditions. We observed a progressive increase in the rate of phosphopeptide formation during the incubation (Figure 2). The initial velocity, approximated from the first time points, was ~4 mol of phosphopeptide/(mol of KD min) compared to an apparent steady-state velocity of ~42 mol/(mol min). The lag period between the low initial rate and the faster steady-state rate can be characterized by an induction time derived from steady-state data extrapolated to "zero turnovers" as marked in Figure 2 by the arrowhead. Preincubation of 50 nM KD with 0.5 mM ATP and 50 mM $MgAc_2$ yielded approximately the same steady-state rate of peptide phosphorylation in a subsequent reaction at 5 nM KD, but without the lag period. Preincubation with the ATP analogue, AMP−PNP, which does not support phosphoryl transfer, did not eliminate the lag period, suggesting that phosphorylation of the KD was required to eliminate the lag period before steady-state peptide phosphorylation was achieved. Furthermore, any mixture of reaction components that did not support autophosphorylation in the preincubation also did not eliminate the lag period in the final reaction. To determine if the apparent steady-state rate of peptide phosphorylation was maximal or not, KD was preincubated with $MgAc_2$ and ATP in the presence of protamine or at very high KD concentrations, either of which promotes activation and trans-autophosphorylation of the AL (*34*, *49*). The low level of protamine in the second incubation had no effect on the rate of peptide substrate phosphorylation (not shown). The rate of peptide phosphorylation after these preincubations was ~310 mol/(mol min). This is roughly 7-fold greater than

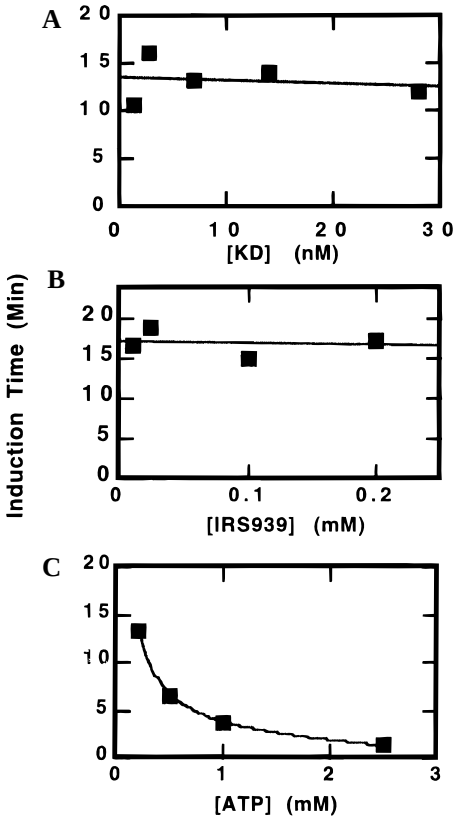

FIGURE 3: Induction time under varied reaction conditions. Peptide phosphorylation was assayed as in Figure 2, with variations in kinase domain, peptide, or ATP concentrations. The induction time was determined by extrapolation of the apparent partially activated steady-state data to 0 turnovers as illustrated in Figure 2. (panel A) Variable kinase domain concentrations between 1.4 and 28 nM. The assays were done at 0.1 mM IRS939 and 0.2 mM ATP. (panel B) Variable peptide substrate concentrations between 0.01 and 0.2 mM IRS939. The assays were done at 2 or 10 nM KD and 0.2 mM ATP. (panel C) Variable ATP concentrations between 0.2 and 1 mM. The assays were done at 20 nM KD and 0.1 mM IRS939.

the apparent steady-state rate observed at very low KD concentrations, and indicates that activation obtained under cis-autophosphorylation reaction conditions was only partial and not maximal.

Since the induction of partial activation depended on autophosphorylation, we tested the effects of varied reaction conditions on the transition. As shown in Figure 3A, the induction time was independent of KD concentration. This is an identifying feature of the cis-autophosphorylation reaction (*34*). The induction time was insensitive to peptide substrate concentration, as seen in Figure 3B. This would be expected since the concentrations employed were well below those needed to obtain significant inhibition of autophosphorylation as demonstrated in Figure 1. Finally, the induction time was shorter at higher ATP concentrations (Figure 3C). While these results are consistent with JM autophosphorylation yielding a partially activated kinase, it is also possible that only a subpopulation of KD was autophosphorylated and activated under these reaction conditions.

Autophosphorylation in the Partially and Fully Activated States. In the partially activated steady state, KD was autophosphorylated at a stoichiometry of 1 mol of phosphate/mol of enzyme (0.8 ± 0.2), determined by recovery of [^{32}P]-phospho-KD after SDS−PAGE. The stoichiometry of

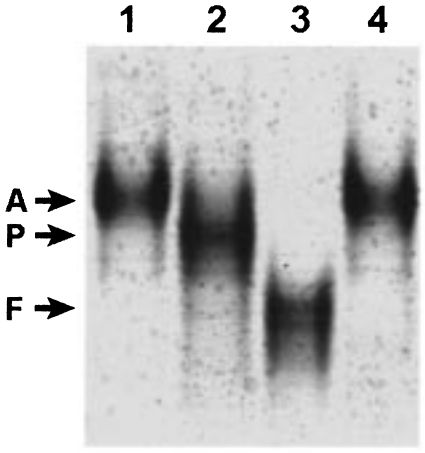

FIGURE 4: Phosphorylation of the kinase domain after partial versus maximal activation. The relative extent of autophosphorylation was analyzed by nondenaturing PAGE and silver staining, with 200 ng/lane of wild-type kinase domain prepared as follows: lanes 1 and 4, without autophosphorylation; lane 2, 0.2 μM KD incubated for 60 min at 0.2 mM ATP, 20 mM $MgAc_2$; lane 3, 2 μM KD incubated for 60 min at 5 mM ATP, 20 mM $MgAc_2$. With respect to peptide substrate phosphorylation rates, these conditions produce the basal-state apoenzyme (A), the enzyme in the partially activated steady state (P), and the fully activated enzyme (F).

autophosphorylation after maximal activation was 5 mol of phosphate/mol of enzyme (5 ± 1 in the absence of protamine, and 3.5 ± 2 in the presence of protamine; the lower value with protamine might have resulted from lower recovery of protein after SDS−PAGE when polycations are present in the original sample; ref *50*). The stoichiometry ≈1 could have resulted from 20% of the KD molecules becoming autophosphorylated to the extent of 5 mol of phosphate/mol of KD, and fewer activated enzymes would have produced a lower rate, comparing the partially and fully activated steady-state rates, respectively (Figure 2). This possibility cannot be ruled out by SDS−PAGE because apoKD and phosphoKD comigrate. However, nondenaturing PAGE can separate multiple phosphoforms of the core KD (*51*). By this method we observed a nearly homogeneous population of purified full-length KD (Figure 4, A). When KD was autophosphorylated under cis-reaction conditions, the KD pool was still homogeneous but displayed a slightly increased electrophoretic mobility (Figure 4, P). After trans-autophosphorylation at a very high KD concentration, the fully activated kinase had a significantly increased mobility in nondenaturing PAGE (Figure 4, F). The apoenzyme mobility was not altered by the presence of reactants, if the reaction was prequenched. This permits us to draw two conclusions:[2] The relative electrophoretic mobilities were consistent with the relative stoichiometries of autophosphorylation. The absence of apoprotein or multiply phosphorylated protein in the partially activated steady state excludes the hypothesis that submaximal enzyme activity resulted from a heterogeneous mixture of inactive apoenzyme and activated phosphoenzymes. Within the limits of resolution and detection,

[2] The simplest interpretation of this experiment is that increased electrophoretic mobilities resulted from increased negative charge due to phosphorylation. Although we cannot rule out contributions from changes in shape (conformation) that would alter the frictional coefficients and therefore the migration, there is not a large enough change in axial ratios of the apo- and tris-phosphorylated core KD calculated from the crystal structures to support this alternative.

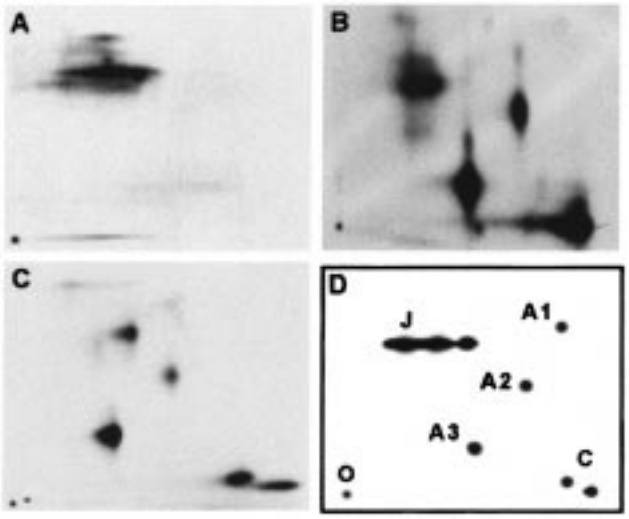

FIGURE 5: Subdomain autophosphorylation of the kinase domain associated with partial versus maximal activation. The sites of autophosphorylation in the wild-type kinase domain were analyzed by two-dimensional [^{32}P]phosphopeptide mapping and autoradiography. Kinase domain was reacted, as indicated below, in the presence of [γ-^{32}P]ATP, resolved by SDS−PAGE, digested with endoproteinase Lys-C, and mapped by thin-layer high-voltage electrophoresis (left-to-right) and chromatography (bottom-to-top), as described in the text. (panel A) After a 60 min reaction of 0.2 μM KD with 0.2 mM [γ-^{32}P]ATP, 20 mM $MgAc_2$, which produces the partially activated steady state of peptide substrate phosphorylation. (panel B) After a reaction of 1 μM KD with 1 mM [γ-^{32}P]-ATP, 20 mM $MgAc_2$, 30 ng of protamine/mL, which produces a maximally activated kinase. (panel C) After a 60 min reaction of 5 μM KD with 5 mM [γ-^{32}P]ATP, 20 mM $MgAc_2$, which produces the maximally activated steady state of peptide substrate phosphorylation. (panel D) Subdomain assignment of the phosphopeptides: J, juxtamembrane; C, carboxy terminus; A, activation loop (-1, -2, -3 phosphates).

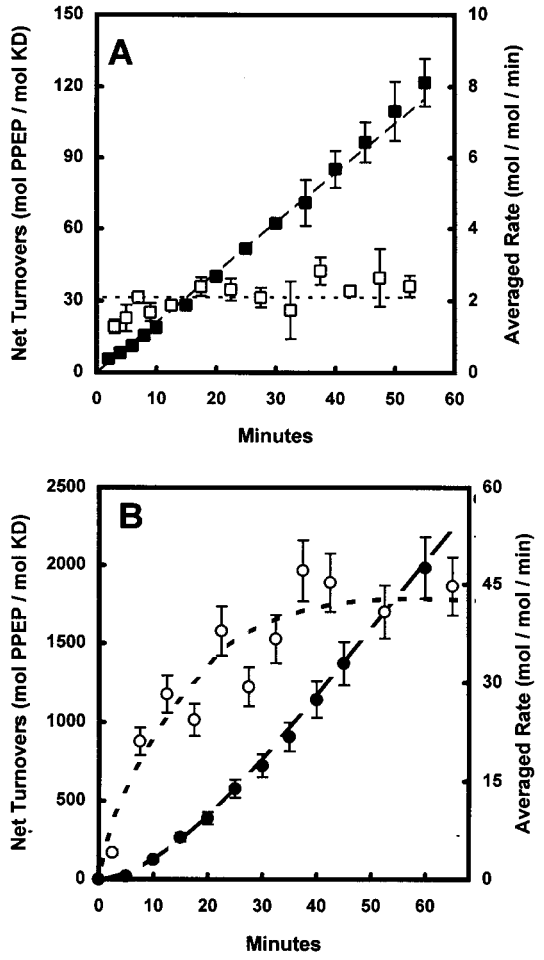

FIGURE 6: Peptide phosphorylation by the JMY2F kinase domain mutant. The phosphorylation of 0.2 mM peptide substrate (IRS939) at 0.2 mM ATP, 20 mM $MgAc_2$, was measured in the presence of 100 nM JMY2F, which has the double Tyr^{965,972}-to-Phe mutation in the juxtamembrane subdomain (panel A), or in the presence of 10 nM wild-type KD (panel B). Both reactions were initiated by the addition of KD. The accumulation of phosphopeptide was monitored in aliquots taken from each incubation, at the times indicated, and plotted as net turnovers (mol of phosphopeptide/mol of KD; solid symbols). The averaged rate of peptide phosphorylation (mol/(mol min); open symbols) was calculated as the difference in net turnovers between successive time points, divided by the difference in time. The dashed lines in panel A are from the data fitted by linear regression, and in Panel B they represent theoretical progress curves, as described in the text. The scales for each panel are different.

all kinase domain molecules appeared to carry one phosphate in the partially activated steady state.

The sites of autophosphorylation were determined for these homogeneous populations of phosphoKD using two-dimensional [^{32}P]phophopeptide mapping (Figure 5). Autophosphorylation in the JM region was observed under conditions that yielded partially activated kinase (Figure 5A). In contrast, maximally activated kinase autophosphorylated to stoichiometries of 3.5 with protamine or to 5 mol of phosphate/mol of KD without protamine, and showed substantial bis- and tris-autophosphorylation in the AL region in addition to JM and CT autophosphorylation (Figure 5B,C). Therefore, the single population of autophosphorylated KD present in the partially activated steady state mapped to the JM region of the insulin receptor's kinase domain.

Substrate Phosphorylation by the JMY2F (Tyr$^{965/972}$Phe) Mutant. On the basis of these results, we concluded that JM autophosphorylation must be avoided if we are to obtain basal-state kinetic parameters and achieve a better understanding of basal-state conformers. Furthermore, the only practical method for eliminating JM autophosphorylation would be Tyr-to-Phe mutations in the JM region because peptide substrate concentrations cannot be raised sufficiently to inhibit cis-autophosphorylation in the wild-type KD (Figure 1). Also, saturating concentrations would not permit evaluation of the Michaelis constant for peptide substrates. Therefore, we tested the *in*ability of the JMY2F (Tyr$^{965/972}$Phe) double mutant to achieve partial activation during coincubation with peptide substrate (Figure 6). In comparison to the wild-type enzyme, a higher concentration of JMY2F was required to observe product formation as indicated by the 20-fold difference in scales for the *y*-axes (Figure 6A versus B). Significantly, the averaged rate of peptide substrate phosphorylation was virtually unchanged over the progress curve with JMY2F, remaining at 2.1 ± 0.6 mol/(mol min) (Figure 6A). This is in striking contrast to the >10-fold rate increase over the progress curve with wild-type KD, and the higher steady-state rate of 45 ± 4 mol/(mol min) (Figure 6B). Therefore, initial velocity measurements for steady-state kinetics in the basal state would be made without preincubation of JMY2F, and the partially activated state would be analyzed after a preincubation of the wild-type KD to achieve stoichiometric cis-autophosphorylation.

Summarizing the observations presented to this point, we conclude that JM autophosphorylation is the underlying molecular basis for partial activation of this kinase: (1) Partial activation resulted from reaction conditions compatible with cis-autophosphorylation (Figure 2). (2) This autophosphorylation mapped to the JM region, and AL autophosphorylation was absent (Figure 5). (3) Partial activation did not occur in the JM Tyr-to-Phe double mutant (Figure 6). In addition, peptide substrates were weak inhibitors of autophosphorylation under these cis-reaction (JM reactive) conditions, as shown in Figure 1. Therefore, in terms of maintaining the apoenzyme during peptide phosphorylation reactions, the best approximation of the basal-state kinase is the JMY2F mutant.

Kinetic Parameters of Basal and Partially Activated Kinase. Determining which kinetic parameters changed during partial activation provides insight into the basal and partially activated states of the kinase. However, extracting basal-state kinetic parameters by curve fitting of the progress curves using wild-type KD is very inexact for several reasons: (1) Fitting the data for net velocity is insensitive to the basal-state contribution within the limits of experimental error. That is, if the basal state contributes $\leq$10% of the net turnovers during the lag period, we cannot distinguish between that level of activity and a basal-state rate of 0. (2) Product accumulation is extremely low at the early time points because the basal state has poor catalytic efficiency. To determine how poor an enzyme the basal-state KD is, higher KD concentrations would be required to increase the number of turnovers at early time points and thereby improve the accuracy of the data. This approach will not work for a single progress curve because pseudo-first-order conditions cannot be maintained at later time points as the substrate concentration falls toward 0. Also higher KD concentrations yield greater trans-autophosphorylation at longer times, and therefore, the apparent steady state would include contributions from AL as well as JM autophosphorylation. (3) Cis-autophosphorylation kinetics are such that very few data points can be collected in which the basal state would contribute most of the turnovers, except at the lower end of the ATP concentration range where the cis-reaction is slowest. This also decreases the accuracy because fewer turnovers of peptide substrate would occur. Therefore, standard initial velocity experiments were done using the JMY2F KD as representative of the basal-state apoenzyme. Wild-type KD autophosphorylated in the JM region (see Figure 5A) yielded the partially activated enzyme.

The kinetic parameters for peptide substrate phosphorylation in the basal and partially activated states are summarized in Table 1. The maximum turnover number of 180 min^{-1} for the basal-state enzyme is the upper estimate. This uncertainty in the basal state "V_{max}" reflects the difficulties encountered in reaching saturation as indicated by the high Michaelis constants for both peptide substrate and ATP. The $K_{M,ATP} \approx 1$ mM measured in the peptide substrate phosphorylation assays fits with the $K^{jm}_{M,ATP} \approx 1$ mM for JM autophosphorylation. The observation that $K_{M,ATP}$ appears unchanged between the wild-type KD and JMY2F in these two assays suggests that the double-point mutation did not in itself alter this kinetic parameter. This is similar to the finding of Backer et al. (*53*) that the $Y^{972}F$ single-point mutation did not change $K_{M,ATP}$ for autophosphorylation although this parameter was increased by internal deletion of 12 residues, $A^{966}-D^{977}$.

Table 1: Kinetic Parameters of Basal and Partially Activated Kinase[a]

KD	k_{cat} (min^{-1})	$K_{M,PEP}$ (mM)	$K_{M,ATP}$ (mM)
JMY2F	180	2.5 ± 1.0	0.9 ± 0.2
jmΠ-WT	600 ± 100	0.2 ± 0.05	1.0 ± 0.2

[a] Steady-state initial velocity measurements of IRS939 (peptide substrate) phosphorylation were done using apo-JMY2F-KD as the "basal state" kinase and JM-autophosphorylated WT-KD (jmΠ-WT) as the "partially activated" kinase. The latter was formed by a 90 min reaction of 0.2 μM KD in 0.2 mM ATP and 20 mM $MgAc_2$, as described under Experimental Procedures. The basal-state reactions were done at 0.2, 0.5, and 1 mM IRS939, the partially activated state reactions were done at 0.1, 0.2, 0.4, 0.6, and 0.8 mM IRS939, and reactions in both states were done at 0.5, 1, 2, and 5 mM ATP (50 mM MgAc). The parameters are averages from both Lineweaver−Burk and Eadie−Scatchard primary and secondary plots of the data.

Evidence from Figure 1 and Table 1 provides a consistent picture of the basal state's weak interaction with peptide substrates. The $K_{M,PEP} \geq 2.5$ mM is a lower limit, but this weak interaction between peptide and the basal-state KD is supported by the $K_i \geq 1$ mM observed for this same peptide against JM autophosphorylation (Figure 1), which also measured an interaction of peptide substrate with the basal-state apoenzyme. The partially activated steady state is due mostly to the >10-fold decrease in the $K_{M,PEP}$ (Table 1). The simplest explanation for this phenomenon is that the JM region blocks peptide substrate binding in the basal state, and JM autophosphorylation relieves this inhibition.

The parameters determined by this analysis, together with the kinetics of cis-autophosphorylation (*34*), can be used to describe the progress curves even under conditions where most of the peptide substrate is converted to product. To generate progress curves from steady-state kinetic parameters we used the following approach. The fraction of KD remaining in the basal state after any elapsed time of reaction is described by the integrated rate equation for a reaction that is zero-order in KD concentration (cis-reaction) but first-order and saturable in ATP concentration,

$$F_b = \exp(-tk_{obs}) \quad (1A)$$

$$k_{obs} = \frac{k_{obs}[ATP]}{K^{jm}_{M,ATP} + [ATP]} \quad (1B)$$

where t is time of reaction in minutes. The ATP dependence of the rate constant for JM autophosphorylation, k_{obs}, is described by eq 1B: k_{jm} is the intrinsic rate constant for JM autophosphorylation ($\sim$0.35 min^{-1}), and $K^{jm}_{M,ATP}$ is the ATP concentration at which the rate of JM autophosphorylation is half-maximal ($\sim$1 mM). The fraction in the basal state varies between 1 at the start of the reaction ($t = 0$) and 0 at infinite time, and the conservation of mass yields the fraction of kinase in the partially activated state as $1 - F_b$. In practical terms (within experimental error), the partially activated state is achieved after about three half-lives when the remaining basal state constitutes just slightly more than 10% of the total kinase pool. This time is shorter at higher ATP concentrations.

The net rate of peptide phosphorylation can be described as the sum of velocities from the basal and partially activated states, weighted for the fraction of enzyme in each state:

$$v_{net} = F_b v_b + (1 - F_b) v_{pa} \quad (2)$$

where each state is indicated by the subscripted "b" or "pa" for basal and partially activated, respectively. The initial velocity for either basal or partially activated state "X" is given by the generic steady-state equation for a sequential two-substrate mechanism (*52*)

$$v_x = \frac{F_x[E]_T k_{cat,x}[ATP][PEP]}{[PEP]K_{M,ATP} + [ATP]K_{M,PEP} + K_{i,ATP}K_{M,PEP} + [ATP][PEP]} \quad (3)$$

where [ATP] and [PEP] are the substrate concentrations, $[E]_T$ is the total kinase domain concentration and therefore F_x-$[E]_T$ gives the relative concentration of the enzyme in either the basal or partially activated states. Similarly, the kinetic constants are those for the corresponding basal or partially activated states listed in Table 1; K_M's are Michaelis constants and $K_{i,ATP}$ is the dissociation constant for ATP from a binary complex with the enzyme. In theoretical calculations below, we set the value of $K_{i,ATP} = K_{M,ATP}$.

In data presented so far, the lag period is readily seen in plots of net product accumulation (net turnovers) per KD versus time of reaction (Figure 2 or Figure 6B, closed symbols) rather than velocity versus time of reaction (Figure 6B, open symbols), and therefore we divide v_{net} by KD concentration (or $[E]_T$ in eq 3) to convert net velocity to net turnovers. The scale of the *y*-axis in plots of net turnovers versus reaction time will vary depending on KD concentration. This is indicated below in Figure 7 which shows experimental data with the calculated progress curves generated using parameters in Table 1. Calculation of the fitted curves was done for 1 min intervals over the first 20 min and for 2 min intervals thereafter; remaining peptide and ATP concentrations were recalculated for each time point on the basis of net turnovers for the preceding time period which is required to account for the decrease in substrate concentrations over time.[3]

The progress curves using 20 nM KD at 0.1 mM peptide and variable ATP concentration (0.1−1 mM) are shown in Figure 7A. Under these conditions substrate-to-product conversion is complete after 5000 turnovers and therefore 10% conversion would be reached after 500 turnovers. The half-time for JM autophosphorylation is calculated to be 14, 7, and 4.6 min for the reactions started at 0.2, 0.5, and 1 mM ATP, respectively. These are similar to the induction times noted in Figure 3. As noted above, at least three half-times for JM autophosphorylation should pass before the steady state is achieved, which would be 42, 21, and 15 min for these three reaction conditions. It can be seen from the data in Figure 7A that the steady state would be reached after the 10% substrate-to-product conversion limit has been passed. Never the less, the fit between experimental and calculated progress curves is good, and confirms that the ATP dependence for the transition from basal to partially activated states can be described with parameters obtained from the steady-state kinetics.

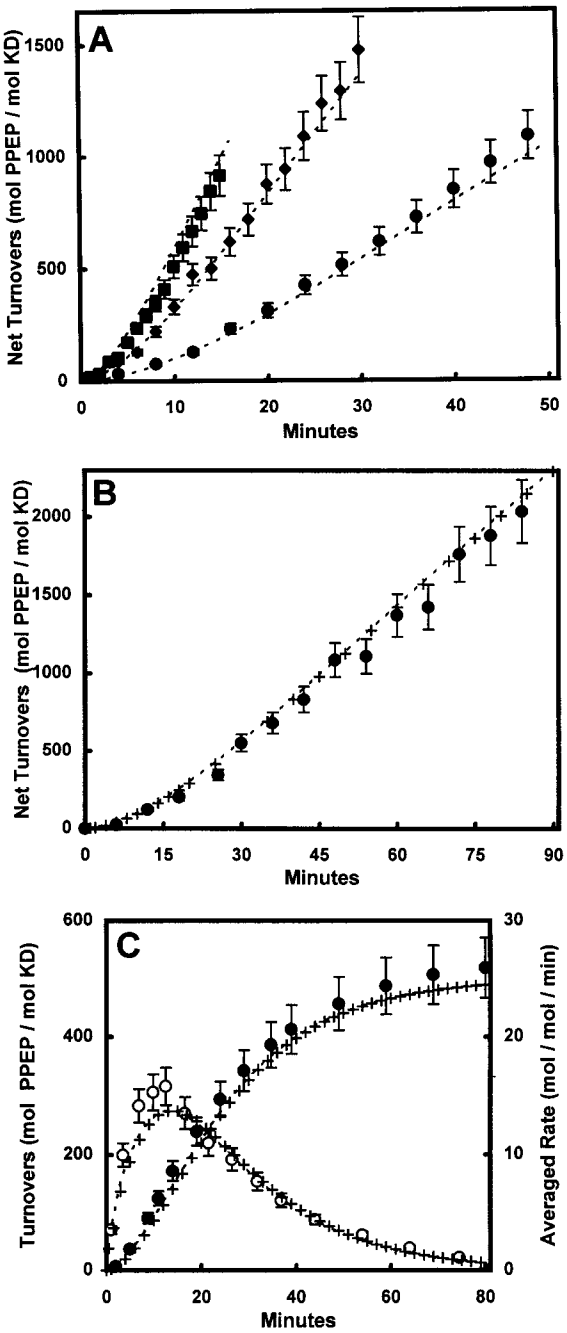

FIGURE 7: ATP and peptide dependence for progressive kinase activation. The progressive increase in peptide substrate phosphorylation rate was analyzed at three ATP concentrations, or at different KD concentrations. The peptide substrate was IRS939. (panel A) Phosphorylation of 0.1 mM IRS939 by 20 nM wild-type KD at 50 mM $MgAc_2$, with 0.2 mM ATP (●), 0.5 mM ATP (◆), 1.0 mM ATP (■). (panel B) Phosphorylation by 6 nM wild-type KD at 50 mM $MgAc_2$, with 0.1 mM IRS939 (●). (panel C) Phosphorylation by 200 nM wild-type KD at 50 mM $MgAc_2$, with 0.1 mM IRS939 (●, turnovers; ○ averaged rate). The dashed lines are theoretical progress curves using the parameters in Table 1, and other parameters for JM autophosphorylation as described in the text. The + symbols show theoretical fits assuming a basal rate of 0.

[3] For example, the rate of product formation between 20 and 22 min was based on the peptide and ATP concentrations remaining at 20 min, and not on the initial reaction conditions. Similarly, the rate between 22 and 24 min was based on the lower reactant concentrations at 22 min, compared to 20 min.

The progress curves extended over longer time periods at 0.1 mM peptide and 0.2 mM ATP are shown in Figure 7, parts B and C, comparing reactions at 6 nM versus 200 nM KD. The substrate-to-product conversion is limited by the peptide concentration and is complete at ~17000 and at 500 net turnovers, respectively, because of the 33-fold difference in KD concentrations employed. These data illustrate the feasibility of obtaining fairly good estimates of the steady-state parameters for the partially activated state only when the net conversion of substrate to product is low during the time required to enter the new steady state. At the lower KD concentration the partially activated steady state is observed after 45 min and seemed to persist at least out to 80 min (one half-time for JM autophosphorylation at 0.2 mM ATP is 14 min). The peptide concentration has fallen only slightly from 100 μM at the start to 95 μM at 45 min and 88 μM at 80 min. The steady-state velocity measured as the slope between 45 and 80 min was measured as 28 mol/(mol min). This is ~20% below the values of 33 mol/(mol min) predicted for these substrate concentrations at 45 min (95 μM peptide and 195 μM ATP) using the steady-state parameters from Table 1. In contrast, at the higher KD concentration there is no apparent steady-state condition because of the more rapidly changing substrate concentration. This is illustrated by the plot of the averaged rate (Figure 7C), which rises and falls over the course of the reaction and barely achieves half of the steady-state rate of 33 mol/(mol min). Although it is possible to obtain reasonably good kinetic data for the partially activated steady state with these assays (Figure 7A,B), the kinetic parameters of the basal state are inaccessible using only the progress curves because of the error inherent in the data at early time points and the reliance on the parameters of the partially activated steady state to fit the early time points. Therefore, the better approximation of basal-state kinetic parameters comes from initial velocity measurements using the JMY2F mutant. That analysis shows that the low catalytic efficiency of the apoenzyme results from an unfavorable Michaelis constant for peptide substrates, and partial kinase activation arose primarily from the improved interaction between the enzyme and peptide substrates.

DISCUSSION

Insulin causes its receptor to switch from a catalytically inefficient basal-state apoenzyme to a maximally activated phosphoenzyme (*54*, *55*). To better understand this transition, the goal of this study was to characterize peptide substrate phosphorylation by the basal-state enzyme. We chose the purified recombinant full-length cytoplasmic kinase domain for this purpose because previous studies showed that autophosphorylation of the KD is a good mimic of native insulin receptor in its basal state (*48*, *56*). It is also known that autophosphorylation of this KD can occur in a pattern and with consequences equivalent to insulin-stimulated native receptor (*48*, *57*), so the activated state's kinetic parameters can be determined as well. Furthermore, the activating autophosphorylation occurs by a trans-reaction (*49*, *58*) which by its nature cannot be avoided in the native IR except by blocking with very high substrate concentrations (*59*, *60*). This restriction precludes analysis of the Michaelis constant for peptide substrate phosphorylation of the apoenzyme. In contrast to the native IR, trans-autophosphorylation by the purified KD can be largely avoided by dilution, leaving only the cis-reaction of juxtamembrane tyrosines (*34*). Whereas AL autophosphorylation and kinase activation could be blocked by substrates, JM autophosphorylation was resistant (Figure 1) and more surprisingly resulted in a partially activated kinase (Figures 2−6). Because this mode of activation could not be avoided in the wild-type KD, and because of limitations in the semicontinuous assay, we concluded that the best approximation of the basal-state apoenzyme would be the double $Tyr^{965/972}$Phe mutant, JMY2F. The inability of JMY2F to display partial activation (Figure 6), and the observation that its low catalytic efficiency was within the boundaries suggested by the semicontinuous assay, permitted this mutant to be used for steady-state peptide phosphorylation kinetics.

The most striking characteristics of the basal state are the extremely unfavorable $K_{M,PEP}$ and the relatively high turnover number. The parameters listed in Table 1 for the apoenzyme, JMY2F, indicate a catalytic efficiency $\leq 7.2 \times 10^4$ M^{-1} min^{-1} which translates into a paucity of allowable turnovers at the expected physiological concentrations of substrates. For example, the basal-state kinase could generate 0.5 turnovers/minute with a polypeptide substrate present at 10 μM in the presence of 3 mM ATP. In contrast the partially activated state with a catalytic efficiency $\leq 3 \times 10^6$ M^{-1} min^{-1} is capable of generating 21 turnovers/min under the same conditions. However for physiological substrates such as IRS, SHC, and Stat5 (*61*) proteins it is well-established that phosphotyrosine-972 in the JM region is an important factor in aiding their phosphorylation (*62*−*65*). The role of JM autophosphorylation in a physiological setting might be dominated by PTB−PY interactions. On the other hand, because peptide phosphorylation studies do not rely on the different PTB−PY interactions, they report independently on factors that affect the active site of the kinase. Therefore, from the change in $K_{M,PEP}$ reported here and by analogy to intrasteric inhibition in other kinases (*66*−*68*), the present study on the apoenzyme indicates that the JM region is an intrasteric inhibitor blocking the active site in the kinase domain's basal state.

In other studies on peptide interactions with the IR, Shoelson et al. (*60*) determined an $IC_{50} \approx 1$ mM against insulin stimulated autophosphorylation but a K_M of ≈0.2 mM as a substrate after insulin-stimulated autophosphorylation.[4] This suggests an improved interaction between the IR and peptide substrates resulting from insulin-stimulated autophosphorylation, which would have been predominantly in the AL (*59*). A similar finding was made by Pike and colleagues (*69*) who showed a high $K_{M,PEP} \approx 2$ mM without prior autophosphorylation of the holoreceptor but a 5-fold decrease in $K_{M,PEP}$ as a consequence of insulin-stimulated autophosphorylation. Furthermore, although not stated explicitly, one can extract a 2−4-fold increase in V_{max} from their data (Walker et al. (*69*) Figure 1 vs Figure 2). Those results would yield a 20-fold increase in catalytic efficiency due to insulin-stimulated autophosphorylation. However, Pike and co-workers did not make a detailed analysis of the unphosphorylated enzyme because of the observed irregular kinetics which could have been due to autophosphorylation

[4] The peptide substrate IRS939 has a K_M ~30 μM with the fully activated wild-type KD (RAK, unpublished data).

coinciding with peptide substrate phosphorylation. From our results on the decrease in $K_{M,PEP}$ due to JM autophosphorylation, which does coincide with peptide phosphorylation, it is reasonable to conclude that the differences observed by Shoelson et al. (*60*) and by Walker et al. (*69*) underestimate the contribution of AL autophosphorylation to activation, and may not fully represent the changes in kinetic parameters. In fact, prior to Walker et al. (*69*), all studies claimed that kinase activation by insulin-stimulated autophosphorylation resulted from changes only in V_{max} and not in $K_{M,PEP}$ (*70*−*73*). In light of the differences in structure between the apo- and tris-phosphorylated IR KD (*74*, *75*), additional changes in $K_{M,PEP}$ and $K_{M,ATP}$ would certainly be expected, and preliminary evidence supports that (Kohanski, unpublished data).

We can speculate on the possible significance of the JM region's cis-inhibitory effect for activation of the native receptor. Previous studies have shown both cis- and trans-autophosphorylation reactions by the insulin receptor (*76*−*78*). According to Pessin the dominant negative effect of one kinase-minus partner in the holoreceptor is that trans-phosphorylation of the kinase-minus β subunit does not activate it and does not lead to reciprocal trans-phosphorylation and activation of the functional subunit (*77*). Their report also showed cis-autophosphorylation in the active subunit of the chimeric IR. Although this was not mapped it should be due to JM autophosphorylation, which we have shown to react by a cis-mechanism (*34*). Shoelson and colleagues have shown asymmetric autophosphorylation in the native IR, interpreted as one β-subunit responding to insulin which then phosphorylates the other β-subunit, which in turn phosphorylates the first subunit (*76*, *78*). While they had not yet demonstrated JM autophosphorylation, their mapping protocol was later shown to identify JM autophosphorylation sites (*35*). In the context of asymmetric autophosphorylation, the first response to insulin might be release of the JM region of the first subunit, which causes release from the cis-inhibited conformer and, by lowering the K_M, increases the efficiency for trans-phosphorylation of the other subunit. Considering the volume two cytoplasmic kinase domains occupy,[5] their respective concentrations may be in the 0.1−2 mM range in the native holoreceptor. Therefore, a K_M for peptide substrates greater than 2.5 mM would severely inhibit phosphorylation of a substrate present even at submillimolar concentrations. The consequence of a ≥10-fold drop in K_M would be a substantially improved rate of trans-phosphorylation. As a time frame for this model of activation, we know that insulin-stimulated receptor autophosphorylation reaches its maximal steady-state level within 1 min in whole cells (*79*). Extrapolating from kinetic parameters in Table 1, and assuming an intracellular ATP concentration of 3 mM, we can calculate 3.5−15 turnovers/min in the basal state and 100−215 turnovers/min in the partially activated state, where the substrate to be phosphorylated is the "other" cytoplasmic kinase domain at 0.1−0.5 mM. This 15−30-fold change in the efficiency of an initial trans-phosphorylation event corresponds to the 20-fold net increase in trans-reactivity predicted from the kinetics of native receptor autophosphorylation (*48*). This increase should permit the kinase to overcome counter-regulatory effects of phosphotyrosine phosphatases such as LAR that might be closely associated with the IR (*80*). We further assume that cis-autophosphorylation is advantageous but not obligatory because JM Tyr-to-Phe mutations do not prevent insulin-stimulated kinase activation (*60*, *62*, *81*). Furthermore, cis-autophosphorylation occurs at a very low rate; given a turnover number of 0.35 min^{-1}, it is 500-fold slower than the maximum turnover number for peptide (trans-) phosphorylation. Again from the perspective of PTPase action, this very low rate for cis-autophosphorylation suggests that the IR can be easily maintained in its unphosphorylated basal state in its normal cellular environment. Even though its kinase domains are constitutively in close proximity, the cis-inhibitory effect of the JM region could in principle easily maintain the IR in its unphosphorylated state.

This mode of intrasteric regulation by the JM region may be specifically important for the small family of "predimerized" receptors such as the insulin and insulin-like growth factor 1 receptors. In these receptors, one other feature of the juxtamembrane region is likely to be especially important. The juxtamembrane region is "tethered" to the plasma membrane, and this will certainly influence the interactions between the JM region and the catalytic core and between the JM regions of the two β-subunits. While the present study has not addressed this experimentally, future studies will focus on this issue directly. Nevertheless, to establish the consequences of cis-autophosphorylation, it was necessary to employ the kinase domain freed from its predimerized environment. Similarly, among established cis-autophosphorylation events, only a few have associated functional consequences. For example, autophosphorylation at Ser10 of porcine heart C subunit of PKA reaches a stoichiometry of 1 but has no effect on the catalytic activity of class-II R subunit association (*82*). Cis-autophosphorylation of ERK1 occurred at a site different from the activation loop but was without any detectable effect on kinase function and furthermore was at a stoichiometry <0.003 (*83*). On the other hand, cis-autophosphorylation at Thr306 of CamK II has an inhibitory effect on activation by Ca^{2+}/CaM, although this reaction can also occur in trans and is in the carboxy-terminal region of the enzyme (*84*). The cis-autophosphorylation of cGK Iβ in the amino-terminal region activates the basal-state enzyme by relief of intrasteric inhibition (*85*) which is functionally most similar to the case we have presented here. Thus, while many of the consequences for cis-autophosphorylations remain cryptic, they occur in regions outside of the activation loop.

In those kinases where reversible AL phosphorylation occurs, phosphorylation in the core-flanking regions has the ability to regulate it. This is certainly true in the cSrc kinase family. As demonstrated recently with Hck (*6*), the cis-inhibitory interaction between the C-terminal phosphoty-

[5] We calculated the volume occupied by two kinase domains as follows: The longest dimension in the unit cell of the crystal structure of the apo-KD core (73) was ~90 Å as listed on the cover page of the 1irk.pdb file available from the Brookhaven Protein Data Bank. The JM "tether" between the core and the inner face of the plasma membrane may be less than or equal to this length. A hemisphere would then be available to the KD, bordered by the inner surface of the plasma membrane and having a radius between 90 and 180 Å. One such hemisphere would have a volume between 0.15 and 1.2×10^{-20} L. When occupied by one KD molecule ($\approx 1.7 \times 10^{-23}$ mol) the concentration would vary between 0.1 and 1.2 mM. If the kinase domains' hemispheres do not overlap, then the concentration is in this range, and if they overlap entirely, the concentration would be doubled.

rosine and the N-terminal SH2 domain not only inhibits the kinase but also inhibits phosphorylation of the activation loop tyrosine. Similarly the N-terminal SH3 domain also inhibits AL phosphorylation. Together these two domains buffer against activation unless the appropriate input stimulus is of sufficient duration or intensity to raise the level of activating ligand to a competitive level; this may affect the timing of signaling when the same ligand can be used for more than one target or pathway. Importantly these examples indicate that partially activated states of protein kinases are significant. Here we have demonstrated a partially activated state of the IR KD arising from juxtamembrane autophosphorylation.

Additional evidence for regulatory roles of amino-terminal and carboxy-terminal "core-flanking segments" has been presented for other protein kinases (*28*, *86*−*88*). The N-terminal "A-helix" of PKA affects the interaction of the C subunit with the class-I R subunit, and alters the thermal stability of the core although not its intrinsic catalytic activity. Mansour et al. (*89*) showed that a 20 amino acid sequence amino-terminal to the conserved core of MAPK kinase has an inhibitory effect on kinase activity. Although it did not act as a pseudosubstrate inhibitor there was a significant effect of mutations in this segment on the K_M for the protein substrate, which was similar in magnitude to the independent effects on K_M of AL phosphorylation or activating mutations (*90*). However, activating mutations in the N-terminal segment and the AL of MAPK kinase were synergistic in elevating the V_{max} and in lowering the K_M for protein substrate. Further studies on the IR KD will be necessary to determine if there is a similar potential for synergistic activation. Our observation that JM autophosphorylation affects the catalytic efficiency of the insulin receptor's kinase domain fits well within the context of core-flanking regulatory effects, and suggests a new mode of catalytic control in receptor tyrosine kinases.

ACKNOWLEDGMENT

We would like to thank Dr. Imre Wolf for peptide synthesis and purification.

REFERENCES

1. Hanks, S. K., Quinn, A. M., and Hunter, T. (1988) *Science 241*, 42−52.
2. Johnson, L. N., Noble, M. E., and Owen, D. J. (1996) *Cell 85*, 149−158.
3. Brown, M. T., and Cooper, J. A. (1996) *Biochim. Biophys. Acta 1287*, 121−149.
4. Sicheri, F., Moarefi, I., and Kuriyan, J. (1997) *Nature 385*, 602−609.
5. Donella-Deana, A., Cesaro, L., Ruzzene, M., Brunati, A. M., Marin, O., and Pinna, L. A. (1998) *Biochemistry 37*, 1438−1446.
6. Moarefi, I., LaFevre Bernt, M., Sicheri, F., Huse, M., Lee, C. H., Kuriyan, J., and Miller, W. T. (1997) *Nature 385*, 650−653.
7. Sabe, H., Knudsen, B., Okada, M., Nada, S., Nakagawa, H., and Hanafusa, H. (1992) *Proc. Natl. Acad. Sci. U.S.A. 89*, 2190−2194.
8. Goldberg, J., Nairn, A. C., and Kuriyan, J. (1996) *Cell 84*, 875−887.
9. Cruzalegui, F. H., Kapiloff, M. S., Morfin, J. P., Kemp, B. E., Rosenfeld, M. G., and Means, A. R. (1992) *Proc. Natl. Acad. Sci. U.S.A. 89*, 12127−12131.
10. Haribabu, B., Hook, S. S., Selbert, M. A., Goldstein, E. G., Tomhave, E. D., Edelman, A. M., Snyderman, R., and Means, A. R. (1995) *EMBO J. 14*, 3679−3686.
11. Chin, D., Sloan, D. J., Quiocho, F. A., and Means, A. R. (1997) *J. Biol. Chem. 272*, 5510−5513.
12. Mukherji, S., Brickey, D. A., and Soderling, T. R. (1994) *J. Biol. Chem. 269*, 20733−20738.
13. Brickey, D. A., Bann, J. G., Fong, Y. L., Perrino, L., Brennan, R. G., and Soderling, T. R. (1994) *J. Biol. Chem. 269*, 29047−29054.
14. Smith, M. K., Colbran, R. J., Brickey, D. A., and Soderling, T. R. (1992) *J. Biol. Chem. 267*, 1761−1768.
15. Soderling, T. R. (1993) *Mol. Cell. Biochem. 127*−*128*, 93−101.
16. Selbert, M. A., Anderson, K. A., Huang, Q. H., Goldstein, E. G., Means, A. R., and Edelman, A. M. (1995) *J. Biol. Chem. 270*, 17616−17621.
17. Hawley, S. A., Selbert, M. A., Goldstein, E. G., Edelman, A. M., Carling, D., and Hardie, D. G. (1995) *J. Biol. Chem. 270*, 27186−27191.
18. Edelman, A. M., Mitchelhill, K. I., Selbert, M. A., Anderson, K. A., Hook, S. S., Stapleton, D., Goldstein, E. G., Means, A. R., and Kemp, B. E. (1996) *J. Biol. Chem. 271*, 10806−10810.
19. Beebe, S. J., and Corbin, J. D. (1986) in *The Enzymes: Control by Phosphorylation, Part A, vol 17* (Boyer, P. D., and Krebs, E. G. Eds.) pp 43−111, Academic Press, New York.
20. Whitehouse, S., and Walsh, D. A. (1983) *Methods Enzymol. 99*, 80−93.
21. Gibbs, C. S., Knighton, D. R., Sowadski, J. M., Taylor, S. S., and Zoller, M. J. (1992) *J. Biol. Chem. 267*, 4806−4814.
22. Knighton, D. R., Zheng, J., Eyck, L. F. T., Ashford, V. A., Xuong, N.-H., Taylor, S. S., and Sowadski, J. M. (1991) *Science 253*, 407−414.
23. Knighton, D. R., Zheng, J., Eyck, L. F. T., Xuong, N.-H., Taylor, S. S., and Sowadski, J. M. (1991) *Science 253*, 414−420.
24. Adams, J. A., McGlone, M. L., Gibson, R., and Taylor, S. S. (1995) *Biochemistry 34*, 2447−2454.
25. Wen, W., and Taylor, S. S. (1994) *J. Biol. Chem. 269*, 8423−8430.
26. Steinberg, R. A., Cauthron, R. D., Symcox, M. M., and Shuntoh, H. (1993) *Mol. Cell. Biol. 13*, 2332−2341.
27. Zheng, J., Knighton, D. R., Xuong, N. H., Taylor, S. S., Sowadski, J. M., and Ten Eyck, L. F. (1993) *Protein Sci. 2*, 1559−1573.
28. Herberg, F. W., Zimmermann, B., McGlone, M. L., and Taylor, S. S. (1997) *Protein Sci. 6*, 569−579.
29. Chestukhin, A., Litovchick, L., Schourov, D., Cox, S., Taylor, S. S., and Shaltiel, S. (1996) *J. Biol. Chem. 271*, 10175−10182.
30. Prigent, S. A., Stanley, K. K., and Siddle, K. (1990) *J. Biol. Chem. 265*, 9970−9977.
31. Herrera, R., and Rosen, O. M. (1986) *J. Biol. Chem. 261*, 11980−11985.
32. Waugh, S. M., and Pilch, P. F. (1989) *Biochemistry 28*, 2722−2727.
33. Schenker, E., and Kohanski, R. A. (1988) *Biochem. Biophys. Res. Commun. 157*, 140−145.
34. Cann, A. D., and Kohanski, R. A. (1997) *Biochemistry 36*, 7681−7689.
35. Feener, E. P., Backer, J. M., King, G. L., Wilden, P. A., Sun, X. J., Kahn, C. R., and White, M. F. (1993) *J. Biol. Chem. 268*, 11256−11264.
36. Kohanski, R. A. (1993) *Biochemistry 32*, 5773−5780.
37. Walseth, T. F., and Johnson, R. A. (1979) *Biochim. Biophys. Acta 562*, 11−31.
38. Palmer, J. L., and Avruch, J. (1981) *Anal. Biochem. 116*, 372−373.
39. Villalba, M., Wente, S. R., Russell, D. S., Ahn, J. C., Reichelderfer, C. F., and Rosen, O. M. (1989) *Proc. Natl. Acad. Sci. U.S.A. 86*, 7848−7852.
40. Ebina, Y., Ellis, L., Jarnagin, K., Edery, M., Graf, L., Clauser, E., Ou, J., Masiarz, F., Kan, Y. W., Goldfine, I. D., Roth, R. A., and Rutter, W. J. (1985) *Cell 40*, 747−758.

41. Whittaker, J., Okamoto, A. K., Thys, R., Bell, G. I., Steiner, D. F., and Hofmann, C. A. (1987) *Proc. Natl. Acad. Sci. U.S.A. 84*, 5237−5241.
42. Ansörge, W. (1982) in *Electrophoresis '82*, pp 235−242, Walter deGruyter, New York.
43. Laemmli, U. K. (1970) *Nature 227*, 680−685.
44. Cann, A. D., Wolf, I., and Kohanski, R. A. (1997) *Anal. Biochem. 247*, 327−332.
45. Boyle, W. J., van der Geer, P., and Hunter, T. (1991) *Methods Enzymol. 201*, 110−149.
46. Shoelson, S. E., Chatterjee, S., Chaudhuri, M., and White, M. F. (1992) *Proc. Natl. Acad. Sci. U.S.A. 89*, 2027−2031.
47. Pronk, G. J., McGlade, J., Pelicci, G., Pawson, T., and Bos, J. L. (1993) *J. Biol. Chem. 268*, 5748−5753.
48. Kohanski, R. A. (1993) *Biochemistry 32*, 5766−5772.
49. Cobb, M. H., Sang, B. C., Gonzalez, R., Goldsmith, E., and Ellis, L. (1989) *J. Biol. Chem. 264*, 18701−18706.
50. Kohanski, R. A. (1989) *J. Biol. Chem. 264*, 20984−20991.
51. Wei, L., Hubbard, S. R., Hendrickson, W. A., and Ellis, L. (1995) *J. Biol. Chem. 270*, 8122−8130.
52. Dixon, M., and Webb, E. C. (1979) *Enzymes*, Academic Press, New York.
53. Backer, J. M., Schroeder, G. G., Cahill, D. A., Ullrich, A., Siddle, K., and White, M. F. (1991) *Biochemistry 30*, 6366−6372.
54. Kohanski, R. A., and Lane, M. D. (1986) *Biochem. Biophys. Res. Commun. 134*, 1312−1318.
55. Kasuga, M., Fujita Yamaguchi, Y., Blithe, D. L., White, M. F., and Kahn, C. R. (1983) *J. Biol. Chem. 258*, 10973−10980.
56. Kohanski, R. A., and Schenker, E. (1991) *Biochemistry 30*, 2406−2414.
57. Tavare, J. M., Clack, B., and Ellis, L. (1991) *J. Biol. Chem. 266*, 1390−1395.
58. Tozzo, E. ,and Desbuquois, B. (1992) *Diabetes 41*, 1609−1616.
59. Flores-Riveros, J. R., Sibley, E., Kastelic, T., and Lane, M. D. (1989) *J. Biol. Chem. 264*, 21557−21572.
60. Shoelson, S. E., White, M. F., and Kahn, C. R. (1989) *J. Biol. Chem. 264*, 7831−7836.
61. Chen, J., Sadowski, H. B., Kohanski, R. A., and Wang, L. H. (1997) *Proc. Natl. Acad. Sci. U.S.A. 94*, 2295−2300.
62. White, M. F., Livingston, J. N., Backer, J. M., Lauris, V., Dull, T. J., Ullrich, A., and Kahn, C. R. (1988) *Cell 54*, 641−649.
63. Kaburagi, Y., Yamamoto-Honda, R., Tobe, K., Ueki, K., Yachi, M., Akanuma, Y., Stephens, R. M., Kaplan, D., Yazaki, Y., and Kadowaki, T. (1995) *Endocrinology 136*, 3437−3443.
64. Gustafson, T. A., He, W., Craparo, A., Schaub, C. D., and O'Neill, T. J. (1995) *Mol. Cell. Biol. 15*, 2500−2508.
65. Sawka-Verhelle, D., Filloux, C., Tartare Deckert, S., Mothe, I., and Van Obberghen, E. (1997) *Eur. J. Biochem. 250*, 411−417.
66. Smith, J. A., Francis, S. H., and Corbin, J. D. (1993) *Mol. Cell. Biochem. 127−128*, 51−70.
67. Soderling, T. R. (1993) *Biotechnol. Appl. Biochem. 18*, 185−200.
68. Kemp, B. E., and Pearson, R. B. (1991) *Biochim. Biophys. Acta 1094*, 67−76.
69. Walker, D. H., Kuppuswamy, D., Visvanathan, A., and Pike, L. J. (1987) *Biochemistry 26*, 1428−1433.
70. Morrison, B. D., and Pessin, J. E. (1987) *J. Biol. Chem. 262*, 2861−2868.
71. Rosen, O. M., Herrera, R., Olowe, Y., Petruzzelli, L. M., and Cobb, M. H. (1983) *Proc. Natl. Acad. Sci. U.S.A. 80*, 3237−3240.
72. White, M. F., Haring, H.-U., Kasuga, M., and Kahn, C. R. (1984) *J. Biol. Chem. 259*, 255−264.
73. Yu, K. T., and Czech, M. P. (1986) *J. Biol. Chem. 261*, 4715−4722.
74. Hubbard, S. R., Wei, L., Ellis, L., and Hendrickson, W. A. (1994) *Nature 372*, 746−754.
75. Hubbard, S. J. (1997) *EMBO J. 16*, 5572−5581.
76. Shoelson, S. E., Böni-Schnetzler, M., Pilch, P. F., and Kahn, C. R. (1991) *Biochemistry 30*, 7740−7746.
77. Frattali, A. L., Treadway, J. L., and Pessin, J. E. (1992) *J. Biol. Chem. 267*, 19521−19528.
78. Lee, J., O'Hare, T., Pilch, P. F., and Shoelson, S. E. (1993) *J. Biol. Chem. 268*, 4092−4098.
79. Kohanski, R. A., Frost, S. C., and Lane, M. D. (1986) *J. Biol. Chem. 261*, 12272−12281.
80. Ahmad, F., and Goldstein, B. J. (1997) *J. Biol. Chem. 272*, 448−457.
81. Rajagopalan, M., Neidigh, J. L., and McClain, D. A. (1991) *J. Biol. Chem. 266*, 23068−23073.
82. Toner-Webb, J., van Patten, S. M., Walsh, D. A., and Taylor, S. S. (1992) *J. Biol. Chem. 267*, 25174−25180.
83. Robbins, D. J., Zhen, E., Owaki, H., Vanderbilt, C. A., Ebert, D., Geppert, T. D., and Cobb, M. H. (1993) *J. Biol. Chem. 268*, 5097−5106.
84. Mukherji, S., and Soderling, T. R. (1994) *J. Biol. Chem. 269*, 13744−13747.
85. Smith, J. A., Francis, S. H., Walsh, K. A., Kumar, S., and Corbin, J. D. (1996) *J. Biol. Chem. 271*, 20756−20762.
86. Shaltiel, S., Cox, S., and Taylor, S. S. (1998) *Proc. Natl. Acad. Sci. U.S.A. 95*, 484−491.
87. Herberg, F. W., Dostmann, W. R., Zorn, M., Davis, S. J., and Taylor, S. S. (1994) *Biochemistry 33*, 7485−7494.
88. Veron, M., Radzio-Andzelm, E., Tsigelny, I., Ten Eyck, L. F., and Taylor, S. S. (1993) *Proc. Natl. Acad. Sci. U.S.A. 90*, 10618−10622.
89. Mansour, S. J., Matten, W. T., Hermann, A. S., Candia, J. M., Rong, S., Fukasawa, K., Vande Woude, G. F., and Ahn, N. G. (1994) *Science 265*, 966−970.
90. Mansour, S. J., Candia, J. M., Matsuura, J. E., Manning, M. C., and Ahn, N. G. (1996) *Biochemistry 35*, 15529−15536.

BI9809122